Geochemistry, Geophysics, Geosystems®

RESEARCH ARTICLE
10.1029/2022GC010688

Origin of ^{182}W Anomalies in Ocean Island Basalts

Gregory J. Archer[1], Gerrit Budde[1,2], Emily A. Worsham[1,3], Andreas Stracke[4], Matthew G. Jackson[5], and Thorsten Kleine[1,6]

[1]Institut für Planetologie, University of Münster, Münster, Germany, [2]Department of Earth, Environmental and Planetary Sciences, Brown University, Providence, RI, USA, [3]Nuclear and Chemical Sciences Division, Lawrence Livermore National Laboratory, Livermore, CA, USA, [4]Institut für Mineralogie, University of Münster, Münster, Germany, [5]Department of Earth Science, University of California Santa Barbara, Santa Barbara, CA, USA, [6]Max Planck Institute for Solar System Research, Göttingen, Germany

Abstract Ocean island basalts (OIB) show variable ^{182}W deficits that have been attributed to either early differentiation of the mantle or core-mantle interaction. However, ^{182}W variations may also reflect nucleosynthetic isotope heterogeneity inherited from Earth's building material, which would be evident from correlated ^{182}W and ^{183}W anomalies. Some datasets for OIB indeed show hints for such correlated variations, meaning that a nucleosynthetic origin of W isotope anomalies in OIB cannot be excluded. We report high-precision W isotope data for OIB from Samoa and Hawaii, which confirm previously reported ^{182}W deficits for these samples, but also demonstrate that none of these samples have resolvable ^{183}W anomalies. These data therefore rule out a nucleosynthetic origin of the ^{182}W deficits in OIB, which most likely reflect the entrainment of either core material or an overabundance of late-accreted materials within OIB mantle sources. If these processes occurred over Earth's history, they may have also been responsible for shifting the ^{182}W composition of the bulk mantle to its modern-day value. We also report Mo isotope data for some Hawaiian OIB, which reveal no resolved nucleosynthetic Mo isotopic anomalies. This is consistent with inheritance of ^{182}W deficits in OIB from the addition of either core or late-accreted material, but only if these materials have a non-carbonaceous (NC) meteorite-like heritage. As such, these data rule out significant contributions of carbonaceous chondrite (CC)-like materials to either Earth's core or late accretion.

Plain Language Summary Some ocean island basalts (OIB) may contain a record of processes and characteristics of the deepest parts of Earth's mantle, including at the boundary between the iron-rich core and mantle. Like some prior studies, we measured tungsten isotopes within OIB from Hawaii and Samoa, and report that tungsten isotopes in these OIB differ in their characteristics compared to what is observed in modern rocks that are most representative of the upper part of Earth's mantle. One explanation for these tungsten isotope anomalies is that they are a signature of chemical interaction between the core and lower mantle, suggesting that the core 'leaks' into the lower mantle. Another possibility proposed here is that these tungsten isotope anomalies reflect ancient crust that contained dense, meteorite-like materials, which sank to the bottom of the mantle during Earth's early history. Using isotopes of another element, molybdenum, we show that the source(s) of these tungsten isotope anomalies do not contain a significant number of materials that originated from the outer Solar System before being added to Earth during its formation.

Key Points:

- ^{182}W deficits in ocean island basalts are confirmed, but correlated ^{182}W–^{183}W anomalies present in prior datasets are not confirmed
- ^{182}W deficits may reflect core-mantle interaction or an overabundance of late-accreted materials, but not nucleosynthetic effects
- Mo isotope data similar to BSE estimate; W-Mo data rule out significant contribution of CC-like material to Earth's core or late accretion

Supporting Information:

Supporting Information may be found in the online version of this article.

Correspondence to:

G. J. Archer,
archer@uni-muenster.de

Citation:

Archer, G. J., Budde, G., Worsham, E. A., Stracke, A., Jackson, M. G., & Kleine, T. (2023). Origin of ^{182}W anomalies in ocean island basalts. *Geochemistry, Geophysics, Geosystems*, *24*, e2022GC010688. https://doi.org/10.1029/2022GC010688

Received 6 SEP 2022
Accepted 1 FEB 2023

Author Contributions:

Conceptualization: Gregory J. Archer, Thorsten Kleine
Funding acquisition: Thorsten Kleine
Investigation: Gregory J. Archer, Emily A. Worsham
Methodology: Gerrit Budde
Project Administration: Thorsten Kleine
Resources: Andreas Stracke, Matthew G. Jackson, Thorsten Kleine
Supervision: Thorsten Kleine
Validation: Gregory J. Archer, Emily A. Worsham, Thorsten Kleine

1. Introduction

Recent studies have reported deficits in ^{182}W, the decay product of short-lived ^{182}Hf ($t_{1/2}$ = 8.9 Ma), in ocean island basalts (OIB). Some OIB with ^{182}W deficits are associated with mantle plumes that extend to the base of the mantle, the D" layer (e.g., Mundl et al., 2017). Entrained material from the base of the mantle may be transported via mantle plumes to the shallow mantle, where partial melting produces OIB. In principle, observed ^{182}W deficits of OIB may thus be inherited from (a) mantle material that underwent crystal-liquid fractionation during the life-time of ^{182}Hf, that is, within the first 60 Ma of Solar System formation (e.g., Mundl et al., 2017), (b) interaction with the core at any time during Earth's history, with the core having an estimated μ^{182}W value (defined as the part per million deviation of a sample's ^{182}W/^{184}W from a W standard) of *ca.* −220 (e.g., Mundl-Petermeier et al., 2020; Rizo et al., 2019), or (c) a preserved overabundance of late-accreted materials, with an estimated μ^{182}W value also around −200, within mantle material (e.g., Puchtel et al., 2020).

Writing – original draft: Gregory J. Archer
Writing – review & editing: Gregory J. Archer, Gerrit Budde, Emily A. Worsham, Andreas Stracke, Matthew G. Jackson, Thorsten Kleine

All of these interpretations assume that the observed $\mu^{182}W$ deficits in OIB are purely radiogenic in origin, that is, they reflect interaction with a reservoir whose low $\mu^{182}W$ reflects Hf-W fractionation and subsequent ^{182}Hf-decay. However, $\mu^{182}W$ values for OIB in prior datasets are correlated with $\mu^{183}W$ (Figure 1), which is characteristic of nucleosynthetic W isotope variations that arise through the heterogeneous distribution of presolar matter in the solar accretion disk. Such $\mu^{182}W$-$\mu^{183}W$ correlations have been observed, for instance, among components of primitive meteorites (Budde et al., 2016; Burkhardt et al., 2012; Kruijer et al., 2014) and bulk meteorites (Kruijer et al., 2017; Qin et al., 2008; Worsham et al., 2019). Of note, linear regression of the $\mu^{182}W$-$\mu^{183}W$ data for OIB returns a slope that is consistent with that expected for nucleosynthetic isotope variations, and so, taken at face value, the ^{182}W–^{183}W co-variation observed among the OIB could also have a nucleosynthetic origin. Distinguishing between a radiogenic and nucleosynthetic origin of ^{182}W deficits in OIB is important for several reasons. First, a nucleosynthetic origin would essentially rule out a core origin for their ^{182}W deficits because due to the strongly negative $\mu^{182}W$ of Earth's core, mixing between ambient mantle and core material would have produced a $\mu^{182}W$-$\mu^{183}W$ co-variation with much steeper slope. Second, prior studies have shown that Earth incorporated material that remains unsampled among meteorites and compared to meteorites is characterized by an excess in nuclides produced in the slow neutron capture process (*s*-process) of stellar nucleosynthesis (Budde et al., 2019; Burkhardt et al., 2011, 2016, 2021). Of note, the coupled ^{182}W–^{183}W deficits observed among OIB would be consistent with an *s*-process excess (Figure 1), in which case the OIB sources might have preserved a signature of some of Earth's building blocks that are unsampled among meteorites.

Although the OIB revealed correlated $\mu^{182}W$-$\mu^{183}W$ variations, only the $\mu^{182}W$ variations are analytically resolved. The $\mu^{183}W$ values are close to or within the analytical resolution of the data, and thus it is unclear whether there are real $\mu^{183}W$ variations among the OIB, and accordingly, prior studies did not attach any significance to these small variations. However, as nucleosynthetic variations for $\mu^{182}W$ are ∼1.5 larger than for $\mu^{183}W$, a nucleosynthetic origin of the ∼15 ppm ^{182}W deficits in OIB would produce $\mu^{183}W$ anomalies of only ∼10 ppm, which is close to the analytical precision of current W isotope data; that is, the observed ^{182}W deficits in OIB could have a nucleosynthetic origin, even if nucleosynthetic $\mu^{183}W$ anomalies cannot be resolved. This issue is further exacerbated by an analytical artifact that selectively depletes ^{183}W, relative to all other W isotopes. This "analytical ^{183}W effect" has been observed in several high-precision W isotope studies from multiple institutions using various purification procedures, and is more prominent in studies utilizing multicollector-inductively coupled plasma mass spectrometry (MC-ICP-MS; e.g., Cook & Schönbächler, 2016; Kruijer et al., 2012; Willbold et al., 2011) rather than thermal ionization mass spectrometry (TIMS; e.g., Mundl et al., 2017; Mundl-Petermeier et al., 2020; Rizo et al., 2019). Nevertheless, although ^{182}W deficits in OIB have so far only been reported using TIMS, the magnitude of any expected nucleosynthetic ^{183}W variations among OIB is so small and close to the analytical precision of the data that verifying the presence or absence of nucleosynthetic W isotope variations in these samples is not possible with currently available data.

To determine the nature of the ^{182}W–^{183}W correlation in datasets from prior OIB studies, and to assess the possibility of nucleosynthetic W isotope variations, we utilized a recently developed method for correcting the analytical ^{183}W effect (Budde et al., 2022) and obtained high-precision MC-ICP-MS W isotope data for several OIB samples from Hawaii and Samoa, including samples for which previous studies reported correlated ^{182}W–^{183}W deficits. For some of the Hawaiian samples of this study, we also determined Mo isotopic compositions, which, in meteorites, generally show larger, more easily measured nucleosynthetic variations than W. Thus, the Mo isotopic compositions of OIB were used to help assess the origin of observed W isotope variations in the OIB.

2. Samples and Methods

2.1. Samples and Sample Preparation

To establish the empirical parameters for the correction of analytical ^{183}W deficits, several well-characterized geological reference materials (GRMs) were analyzed. These include JA-2 (andesite), JB-2 (basalt), JG-1 (granodiorite), and JR-1 (rhyolite). In addition, several aliquots of mid-ocean ridge basalt (MORB) sample PS66-261 from the Central Lena Trough (see Nauret et al. (2011) for sample description and geochemical characterization), doped with variable amounts (approximately +15 ng to +9,940 ng) of an *Alfa Aesar* W solution standard (batch no. 22312) prior to separation and purification of W, were also analyzed. All GRMs and MORB sample PS66-261 were already available as powders at the University of Münster.

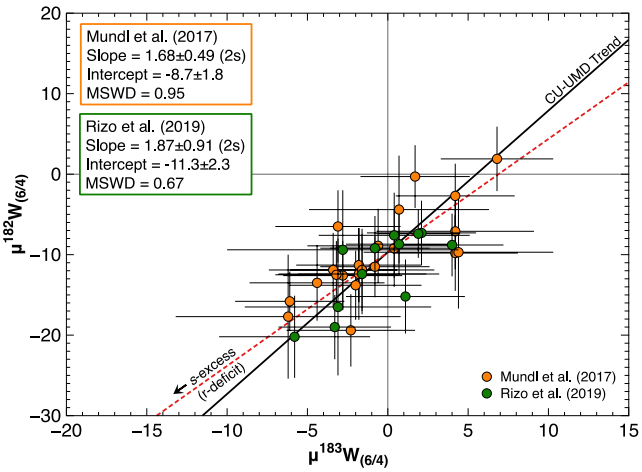

Figure 1. $\mu^{182}W$ (6/4) versus $\mu^{183}W$ (6/4) values for ocean island basalts (OIB) measured by TIMS and reported in prior studies (Mundl et al., 2017; Rizo et al., 2019). Note that only datasets for which $\mu^{183}W$ (6/4) values were reported in prior studies are included. Linear regressions were performed using IsoplotR (Vermeesch, 2018). In a combined regression for data from Mundl et al. (2017) and Rizo et al. (2019), the "CU-UMD" trend is also plotted for comparison. The expected correlation between $\mu^{182}W$ (6/4) and $\mu^{183}W$ (6/4) values for *s*-process nucleosynthetic variation is shown as a red dashed line (Burkhardt & Schönbächler, 2015). The *s*-process line is offset from the origin to pass through the intercept of the OIB data.

Samoan OIB ALIA-115-18 (from Savai'i Island), AVON3-70-9 (from Vailulu'u seamount), AVON3-73-1 (from Vailulu'u seamount), and T33 (from Ta'u Island) were obtained as powders from the University of California Santa Barbara via the University of Maryland. Two other Samoan samples, OFU-04-14 and OFU-05-18 (both from Ofu Island), were provided directly by the University of California Santa Barbara as rock fragments. Sample descriptions, W concentrations, ^{182}W isotopic compositions (measured by TIMS), ^{187}Re-^{187}Os systematics, highly siderophile element (HSE) data, and He isotopic compositions for the Samoan samples examined here have been previously reported by Mundl et al. (2017) and references therein. Hawaiian sample BHVO-2 was available as a powder at the University of Münster, and prior data for BHVO-2 were reported in Kruijer and Kleine (2018). Hawaiian samples KK 16-1, KK 25-4, and Kilauea 1712b were acquired from the Smithsonian Institution as rock fragments. Sample descriptions and He isotopic compositions are reported in Honda et al. (1991) and Kurz et al. (1983). No W isotope data have been reported so far for these Hawaiian samples. The rock fragments were crushed into powders using an agate mortar and pestle at the University of Münster. To avoid contamination, contact with metal tools was avoided, and the agate mortar and pestle were cleaned with quartz sand and Milli-Q water between samples. None of the OIB studied here have been previously analyzed for their mass-independent Mo isotopic composition.

2.2. Analytical Methods

See Supporting Information S1 for detailed descriptions of the analytical method used to separate and purify W. Total procedural blanks for W were <160 pg, and therefore negligible, given that >75 ng W were processed for each sample. Tungsten isotopic compositions were measured using the Thermo Scientific Neptune Plus MC-ICP-MS at the Institut für Planetologie. For W, the instrumental configuration of Kruijer et al. (2015) was used. Data are reported as $\mu^{x}W$ values (part per million deviations from an *Alfa Aesar* W standard, batch no. 22312; Kleine et al., 2002), and are normalized to either $^{186}W/^{184}W = 0.92767$ (denoted "6/4") or $^{186}W/^{183}W = 1.9859$ (denoted "6/3"). Tungsten concentrations were determined by isotope dilution and measured using the above-mentioned MC-ICP-MS instrument (Text S1 in Supporting Information S1).

The analytical methods of Budde et al. (2019) were used to measure Mo. Molybdenum blanks were <5 ng and therefore negligible, as >150 ng Mo were processed for each sample analyzed. For this study, samples were measured using two different cone configurations on the above-mentioned MC-ICP-MS instrument, (a) standard sampler cone paired with an H skimmer cone, and (b) standard sampler cone paired with an X skimmer cone. The standard-X setup improved the sensitivity by a factor of two, and this setup was employed to increase the possible number of measurements. Both setups have been used previously, and both produce data that are in good agreement with one another (Brennecka et al., 2020; Worsham & Kleine, 2021). Molybdenum data are reported as $\varepsilon^{x}Mo$ values (part per ten thousand deviations from an *Alfa Aesar* Mo standard), and are normalized to $^{98}Mo/^{96}Mo = 1.453173$ (Lu & Masuda, 1994).

3. Results

3.1. Tungsten Isotopic Systematics

Tungsten isotopic data for GRMs, as well as MORB PS66-261 doped with an *Alfa Aesar* W standard, are reported in Table 1. Measured $\mu^{182}W$ (6/4) values are ≈0, but $\mu^{183}W$ (6/4) values range from +1.8 to −11.8 (Figure 2). In addition, all $\mu^{x}W$ values that use ^{183}W for internal normalization, including $\mu^{182}W$ (6/3) and $\mu^{184}W$ (6/3), also deviate from 0, with ranges of +16.4 to −3.7, and +7.8 to −1.2, respectively (Figure 2). These coupled W isotope variations are consistent with the analytical ^{183}W effect observed in several prior high-precision W isotope stud-

Table 1
Tungsten Isotopic Compositions of Geological Reference Materials and Doped Mid-Ocean Ridge Basalt PS66-261

			Normalized to $^{186}W/^{184}W = 0.92767$				Normalized to $^{186}W/^{183}W = 1.9859$			
	$W_{initital}$ (ng)	N	$\mu^{182}W_{Meas.}$	±	$\mu^{183}W_{Meas.}$	±	$\mu^{182}W_{Meas.}$	±	$\mu^{184}W_{Meas.}$	±
Geological reference materials										
JG-1	526	8	−0.6	5.0	−8.5	6.5	11.6	4.7	5.7	4.3
JR-1	1,024	13	−1.6	3.0	−7.9	2.8	8.3	2.3	5.3	1.8
JA-2	535	6	−2.2	2.1	−11.5	3.6	12.5	3.8	7.6	2.4
JB-2	154	16	0.4	2.5	−11.8	2.3	16.4	2.4	7.8	1.5
MORB PS66-261 (doped)										
10,000 ng	10,349	6	−0.3	3.6	−1.6	4.0	2.4	5.1	1.0	2.6
5,000 ng	5,165	6	−0.9	5.2	1.8	4.4	−3.7	4.4	−1.2	2.9
2,000 ng	2,073	6	−2.3	3.9	−2.6	3.2	1.1	2.2	1.7	2.3
400 ng	414	6	0.9	5.0	−5.6	5.5	8.5	6.9	3.7	3.6
200 ng	215	6	0.7	4.7	−7.9	5.6	11.5	5.7	5.3	3.8

Note. Data are normalized to either $^{186}W/^{184}W = 0.92767$ or $^{186}W/^{183}W = 1.9859$. $\mu^{18x}W_{Meas.}$ is the measured isotopic deviation of a sample, in parts per million, from an *Alfa Aesar* solution standard, batch no. 22312, which has an indistinguishable W isotopic composition from the NIST3163 standard (Kruijer et al., 2012). The uncertainties are 95% confidence limits of the mean, and were calculated using the equation (s.d. × t0.95, N−1)/$\sqrt{N}$.

ies using MC-ICP-MS (e.g., Cook & Schönbächler, 2016; Kruijer et al., 2012; Willbold et al., 2011). However, consistent with the results of Budde et al. (2022), the magnitude of the observed ^{183}W effect is correlated with the amount of W processed for each standard (Figure 3). This correlation forms the basis for correcting this effect in the new OIB data.

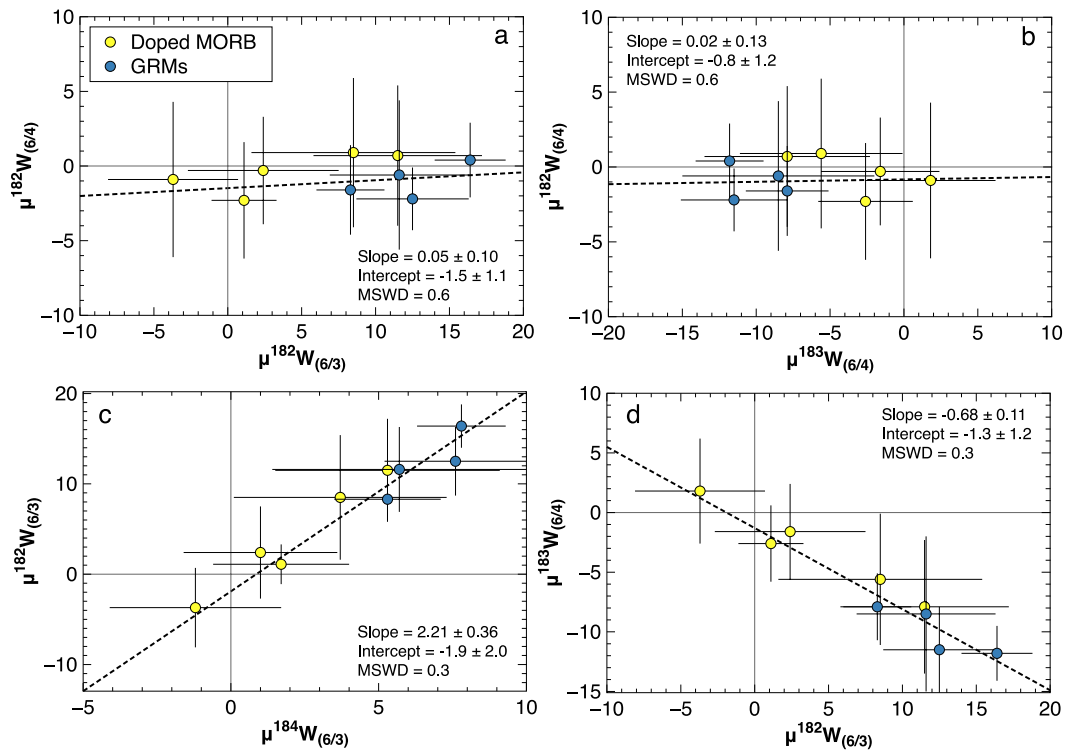

Figure 2. Tungsten isotopic compositions of geological reference materials JB-2, JG-1, JA-2, and JR-1 (blue), as well as mid-ocean ridge basalt sample PS66-261 (yellow) doped with variable amounts of an *Alfa Aesar* W solution standard. Linear regression of the data was performed using IsoplotR (Vermeesch, 2018).

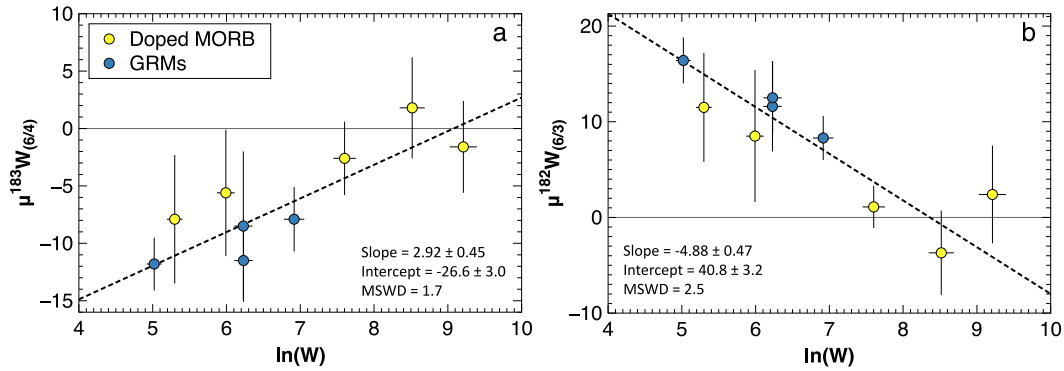

Figure 3. $\mu^{x}W$ values that involve ^{183}W versus ln(W), which is the natural log of the abundance of W (ng/g) processed through the same chemical separation and purification method used for samples. Yellow dots are for mid-ocean ridge basalt sample PS66-261 doped with an *Alfa Aesar* W solution standard. Blue dots are from geological reference materials JB-2, JG-1, JA-2, and JR-1. Linear regressions of the data were performed using IsoplotR (Vermeesch, 2018).

Tungsten isotopic data for Samoan and Hawaiian OIB are reported in Table 2. Measured $\mu^{182}W$ (6/4) values for Hawaiian and Samoan samples range from +1.1 to −17.2 (Figure 4), in agreement with the range of values for Hawaiian and Samoan OIB reported in prior studies (Mundl et al., 2017; Mundl-Petermeier et al., 2020). For particular samples measured both here and in Mundl et al. (2017), $\mu^{182}W$ (6/4) values overlap within uncertainties (Figure 5); however, two of the five samples plot off a 1:1 line. Like the GRMs measured in this study, $\mu^{183}W$ (6/4) deficits are also observed for OIB, and range from −7.0 to −19.2 (Figure 4). These $\mu^{183}W$ (6/4) values are generally lower than previously reported OIB data measured by TIMS (e.g., Mundl et al., 2017; Rizo et al., 2019),

Table 2
Tungsten Isotopic Compositions of Ocean Island Basalts

			Normalized to $^{186}W/^{184}W = 0.92767$						Normalized to $^{186}W/^{183}W = 1.9859$							
	$W_{initital}$ (ng)	N	$\mu^{182}W_{Meas.}$	±	$\mu^{183}W_{Meas.}$	±	$\mu^{183}W_{Corr.}$	±	$\mu^{182}W_{Meas.}$	±	$\mu^{184}W_{Meas.}$	±	$\mu^{182}W_{Corr.}$	±	$\mu^{184}W_{Corr.}$	±
Samoa																
OFU-04-14	107	5	−11.6	4.6	−19.2	8.1	−6.2	8.9	13.5	7.7	12.8	5.4	−4.5	8.6	4.2	5.9
repl.		4	−11.8	9.0	−14.9	4.3	−1.9	5.6	7.7	13.7	9.9	2.9	−10.3	14.2	1.3	3.8
OFU-05-18	207	6	−12.1	3.0	−18.1	4.6	−7.1	6.0	11.8	5.9	12.1	3.0	−3.0	7.2	4.7	3.9
repl.		6	−13.5	5.1	−10.1	8.8	0.9	9.6	−0.4	6.9	6.5	5.5	−15.2	8.0	−0.9	6.0
repl.		6	−13.5	5.1	−12.7	1.8	−1.7	4.2	3.5	3.8	8.3	1.4	−11.3	5.6	0.9	2.9
ALIA 115-18	253	5	1.1	2.7	−11.4	3.7	−1.0	5.4	16.6	5.4	7.6	2.4	2.8	6.8	0.6	3.5
AVON3-70-9	262	6	−3.2	4.1	−12.8	2.9	−2.5	4.9	14.1	3.0	8.5	2.0	0.5	5.1	1.6	3.2
AVON3-73-1	347	6	−0.5	5.4	−9.3	3.9	0.2	5.6	11.9	2.1	6.2	2.6	−0.4	4.7	−0.2	3.7
T33	152	6	−1.9	4.7	−7.0	2.9	4.9	4.7	7.2	1.8	4.6	2.0	−9.1	4.4	−3.3	3.2
Hawaii																
BHVO-2	126	4	−7.1	9.1	−11.3	6.8	1.2	7.7	6.8	11.3	7.5	4.5	−10.4	12.0	−0.8	5.1
repl.		5	−5.6	4.1	−11.9	3.1	0.6	4.8	7.9	8.1	8.6	1.9	−9.3	9.0	0.3	3.1
KK16-1	79	5	−17.2	6.1	−11.8	5.7	2.0	6.7	−1.3	4.9	7.8	3.8	−20.8	6.2	−1.4	4.5
KK 25-4	90	5	−13.1	6.7	−12.6	7.0	0.9	7.9	4.1	8.0	8.4	4.7	−14.8	8.9	−0.6	5.3
Kilauea 1712b	78	6	−5.2	1.4	−16.1	1.6	−2.2	3.9	16.2	2.1	10.7	1.1	−3.4	4.3	1.5	2.6

Note. Data are normalized to either $^{186}W/^{184}W = 0.92767$ or $^{186}W/^{183}W = 1.9859$. $\mu^{18x}W_{Meas.}$ is the measured isotopic deviation of a sample, in parts per million, from an *Alfa Aesar* solution standard, batch no. 22312, which has an indistinguishable W isotopic composition from the NIST3163 standard (Kruijer et al., 2012). $\mu^{18x}W_{Corr.}$ is corrected for an analytical effect that selectively depletes ^{183}W. This correction is based on an empirical relationship between the amount of W processed, and the magnitude of the effect defined by samples and geological reference materials reported in Table 1. Uncertainties associated with corrections for this analytical effect were propagated and reported along with $\mu^{18x}W_{Corr.}$ values. The uncertainties are 95% confidence limits of the mean, and were calculated using the equation (s.d. × $t0.95$, $N-1)/\sqrt{N}$.

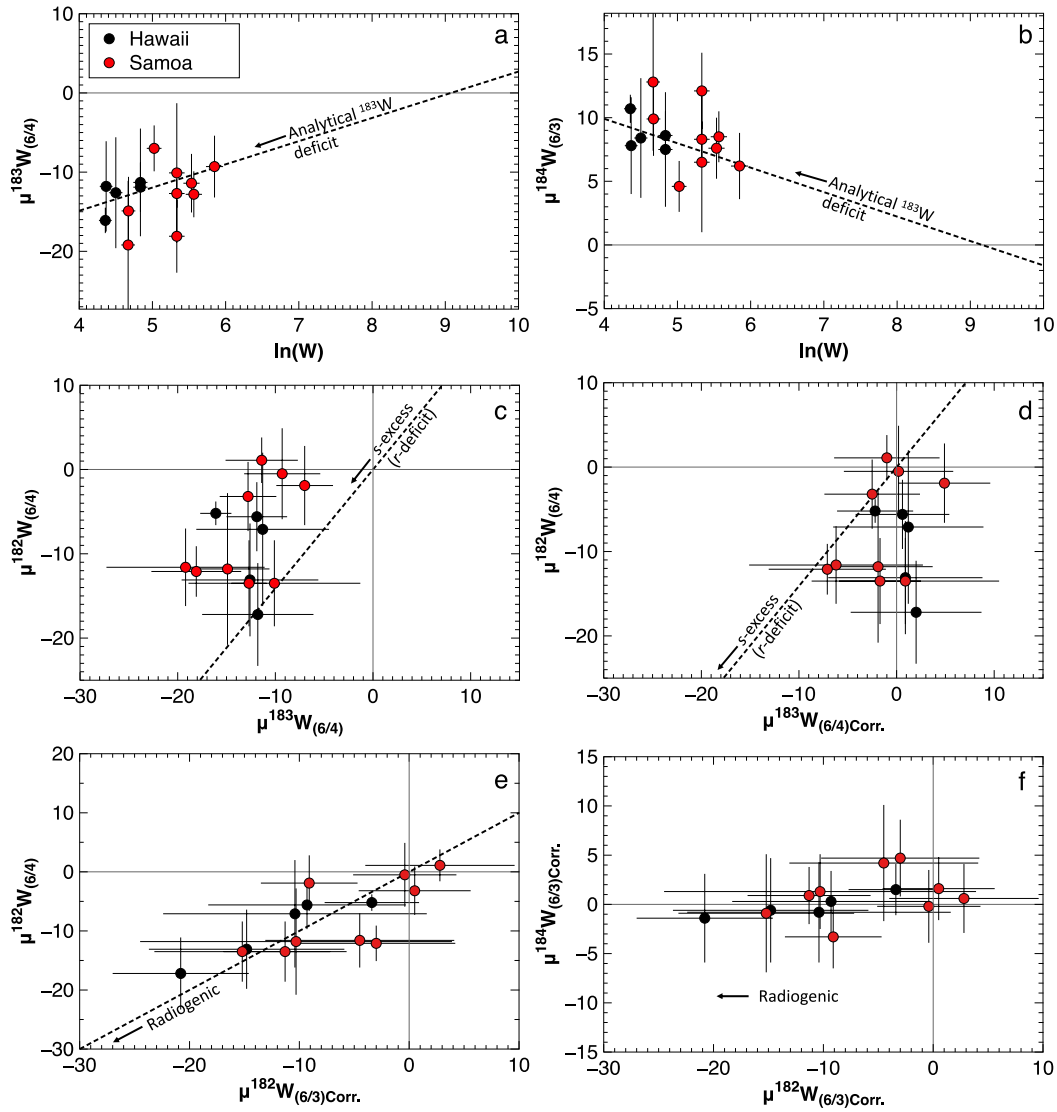

Figure 4. Tungsten isotopic compositions of Hawaiian (black) and Samoan (red) ocean island basalts measured in this study. The $\mu^{x}W_{(6/x)Corr.}$ values are corrected for an analytical effect that only affects isotope ratios that involve ^{183}W. Data do not appear to plot along the expected correlation for *s*-process nucleosynthetic variations (d), indicating that variations in ^{182}W are purely radiogenic in origin. The *s*-process line is from Burkhardt and Schönbächler (2015). Slopes and intercepts for the "analytical ^{183}W deficit" lines were determined from geological reference materials and a doped mid-ocean ridge basalt sample. The radiogenic line in a plot of $\mu^{182}W_{(6/4)}$ versus $\mu^{182}W_{(6/3)Corr.}$ has a slope of 1.

consistent with prior observations that the analytical ^{183}W effect is larger in MC-ICP-MS than in TIMS studies. Similar to W data for GRMs, ^{183}W (6/4) deficits in OIB also manifest as apparent excesses in $\mu^{182}W$ (6/3) and $\mu^{184}W$ (6/3) values, with ranges of +16.6 to −1.3 and + 12.8 to 4.6, respectively (Figure 4). An important difference from prior studies is that in spite of the $\mu^{183}W$ variations, no correlated $\mu^{182}W$-$\mu^{183}W$ variations are observed for the OIB data of this study (Figure 4d).

3.2. Molybdenum Isotopic Systematics

The Mo isotopic compositions of Hawaiian OIB are reported as $\varepsilon^{x}Mo$ and $\Delta^{95}Mo$ values in Table 3. A sample's $\Delta^{95}Mo$ is defined as its ppm deviation from an *s*-process mixing line passing through the origin ($\Delta^{95}Mo = (\varepsilon^{95}Mo - 0.596 \times \varepsilon^{94}Mo) \times 100$), and this value has been used to estimate the relative contributions of non-carbonaceous (NC) and carbonaceous (CC) materials to the BSE's Mo isotopic composition (Budde et al., 2019). The $\varepsilon^{x}Mo$ and

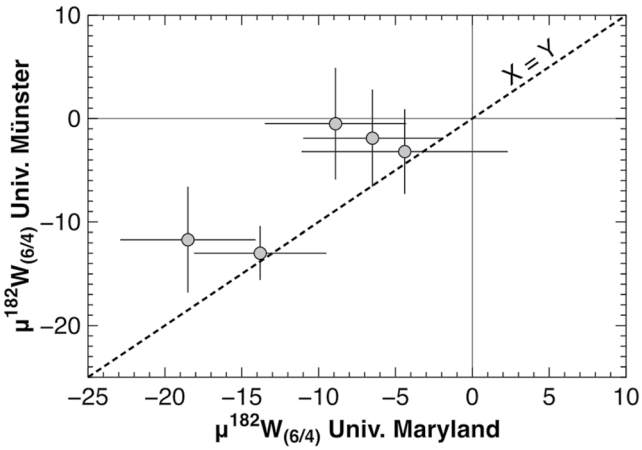

Figure 5. Tungsten isotopic compositions for Samoan samples were measured in both this study (Univ. Münster) and a prior study (Univ. Maryland; Mundl et al., 2017). Samples measured multiple times in either study were averaged and the errors propagated. Note that only samples which have reported μ^{182}W (6/4) and μ^{183}W (6/4) are included; Samoan sample ALIA 115-18 was measured in both studies, but μ^{182}W (6/4) values are not available from Mundl et al. (2017; see supplement).

Δ^{95}Mo values for each sample are indistinguishable within uncertainty from one another with average ε^{94}Mo = 0.02 ± 0.05, ε^{95}Mo = 0.08 ± 0.05, and Δ^{95}Mo = 7 ± 5 (2SD, N = 3), and are also indistinguishable from the BSE as defined by Budde et al. (2019) (ε^{94}Mo = 0.04 ± 0.06, ε^{95}Mo = 0.10 ± 0.04, Δ^{95}Mo = 7 ± 5, 95% CI, N = 5).

4. Discussion

Before examining the combined ^{182}W-Mo data (Section 4.4), it is first necessary to determine the nature of W isotope variations in OIB.

4.1. Correction of Analytically Induced ^{183}W Deficits (i.e., "the ^{183}W Effect")

A persistent issue for high-precision W isotope measurements is the analytical ^{183}W effect, which selectively depletes ^{183}W during separation and purification of W (e.g., Archer et al., 2019; Budde et al., 2022; Cook & Schönbächler, 2016; Kruijer et al., 2012; Takamasa et al., 2020; Willbold et al., 2011). Prior studies proposed that analytical ^{183}W deficits are the result of a nuclear field shift effect (Cook & Schönbächler, 2016), but Budde et al. (2022) showed that this is unlikely to be the cause. Instead, Budde et al. (2022) proposed that ^{183}W deficits may be the result of a magnetic isotope effect. Although the exact cause of the ^{183}W effect is still a matter of debate and beyond the scope of this study, the observation that its magnitude is predominantly a function of the amount of W processed through the chemical separation procedure (Budde et al., 2022) allows for the accurate correction of analytically induced ^{183}W deficits when observed. As the parameters of such regressions are specific to a certain analytical protocol (and possibly even operator), here we use a regression of terrestrial GRMs (JG-1, JR-1, JA-2, and JB-2) and mid-ocean ridge basalt (MORB sample PS66-261) doped with variable amounts of the *Alfa Aesar* W solution standard based on our own data. For more details about analytical ^{183}W deficits and their causes, we refer the reader to Budde et al. (2022).

The slope of linear regression of the natural log of the W abundance, ln(W), versus μ^{183}W (6/4) for the terrestrial GRMs and the doped MORB samples is 2.92 ± 0.45 with an intercept of −26.6 ± 3.0 (Figure 3). For μ^{182}W (6/3), this regression yields a slope of −4.88 ± 0.47 and intercept of 40.8 ± 3.2 (Figure 3). Using these regression parameters and the known amounts of W processed for each OIB, the analytical ^{183}W effect was subtracted from the measured values of OIB. After this correction, 12 out of 14 OIB μ^{183}W values are within uncertainty of the terrestrial standards (μ^{183}W = 0), and μ^{182}W (6/3)-μ^{182}W (6/4) values plot along a 1:1 line (Figure 4). One measurement of OFU-05-18 plots slightly off this line and has a slightly negative μ^{183}W; however, subsequent replicate measurements of OFU-05-18 did not reproduce this apparent anomaly, and thus this offset likely represents an inaccurate correction of the ^{183}W deficit for this particular sample during the initial stages of data acquisition. Note that since the analytical artifact only depletes ^{183}W, and leaves the other W isotopes effectively unchanged, no corrections are necessary for μ^{182}W (6/4). This is consistent with the observation that the terrestrial GRMs and doped MORB are all characterized by measured μ^{182}W (6/4) ≈ 0 (Table 1, Figure 2). Consequently, the 1:1

Table 3
Molybdenum Isotopic Compositions of Ocean Island Basalts

	N	ε^{92}Mo	±	ε^{94}Mo	±	ε^{95}Mo	±	ε^{97}Mo	±	ε^{100}Mo	±	Δ^{95}Mo	±
Hawaii													
KK 16-1	23	0.04	0.09	0.01	0.05	0.05	0.03	0.03	0.03	−0.01	0.03	4.4	4.2
KK 25-4	15	0.12	0.11	0.05	0.07	0.09	0.06	0.05	0.05	−0.02	0.07	6.0	7.3
Kilauea 1712b	24	0.08	0.11	0.01	0.06	0.10	0.04	0.05	0.03	−0.06	0.07	9.4	5.4

Note. Data are reported as ε^{x}Mo values and are normalized to ^{98}Mo/^{96}Mo = 1.453173 (Lu & Masuda, 1994). The uncertainties are the 95% confidence interval of the mean and were calculated using the equation (s.d. × t0.95, N−1)/$\sqrt{N}$.

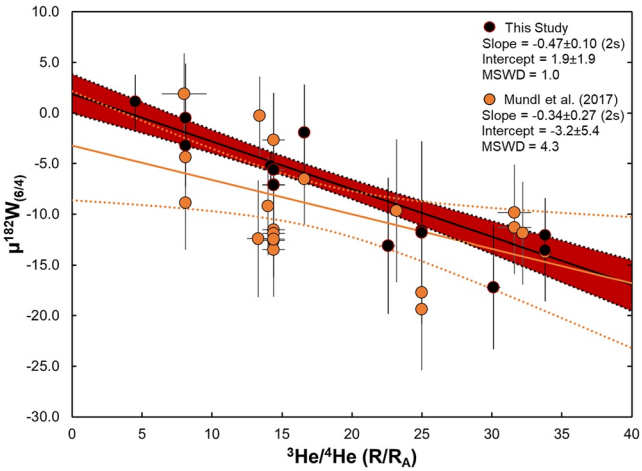

Figure 6. $\mu^{182}W_{(6/4)}$ values versus $^{3}He/^{4}He$ for Hawaiian and Samoan samples from this study and Mundl et al. (2017). Linear regression and error envelopes were calculated using ISOPLOT (Ludwig, 2001), instead of IsoplotR (Vermeesch, 2018), as the latter does not calculate nor display error envelopes. Linear regressions of the data calculated using ISOPLOT and IsoplotR have slopes and intercepts that are in good agreement. The error envelope for samples from this study is bounded by black dotted lines and shaded red. The error envelope for the data from Mundl et al. (2017) is unshaded and bounded by orange dotted lines.

correlation between corrected $\mu^{182}W$ (6/3) and measured $\mu^{182}W$ (6/4) values (Figure 4e) and the observation that after correction, samples have $\mu^{183}W \approx 0$ (Figure 4d) demonstrate the accuracy of the correction method.

4.2. Comparison to Previous Studies

The new W isotope data of this study confirm earlier results that OIB from Hawaii and Samoa are characterized by variable $\mu^{182}W$ deficits. For particular samples measured both in Mundl et al. (2017) and in this study, $\mu^{182}W$ (6/4) values are within uncertainty of each other (Figure 5), although two of the five samples also analyzed by Mundl et al. (2017) plot off a 1:1 line. The results of this study also confirm that ^{182}W deficits in some Hawaiian and Samoan are correlated with $^{3}He/^{4}He$ (Figure 6), as reported in prior studies (e.g., Mundl et al., 2017). Linear regression of the data from Samoa and Hawaii reported here yields a single trend in $^{3}He/^{4}He$ versus $\mu^{182}W$ (6/4) with a somewhat improved fit (MSWD = 1.0) compared to the previously reported data set (MSWD = 4.3; Mundl et al., 2017).

In contrast to prior studies (Mundl et al., 2017; Rizo et al., 2019), however, we do not observe correlated $\mu^{182}W(6/4)$-$\mu^{183}W(6/4)$ variations among the OIB, regardless of whether they are corrected for the ^{183}W effect or not (compare Figure 1 and Figures 4c and 4d). It is important to note that any covariation of $\mu^{182}W$ (6/4) and $\mu^{183}W$ (6/4) cannot be due to the analytical ^{183}W effect described above, which leaves $\mu^{182}W$ (6/4) unaffected. As such, the most likely explanation is that the $\mu^{182}W$ (6/4)-$\mu^{183}W$ (6/4) covariations present in prior datasets for OIB result from residual isotopic correlations during the TIMS measurements. Such correlations have been previously identified in high-precision isotope ratio datasets of several elements (e.g., Ru, W, Nd) measured by TIMS. These have been attributed to uncorrected variations in the evolving O isotopic composition of oxides during measurements (Bermingham et al., 2016), small changes in the sensitivity of faraday cup detectors due to continual degradation over months-long periods (Archer et al., 2017), or changing mass fractionation behavior due to evaporation of multiple domains on a filament (Andreasen & Sharma, 2009).

Despite the variable ^{182}W deficits, all samples reported in this study are characterized by $\mu^{183}W \approx 0$ after correction for the ^{183}W effect and no systematic variation of $\mu^{182}W$ with $\mu^{183}W$ variation is observed (Figure 4d). Thus, in contrast to the data shown in Figure 1, we can rule out a nucleosynthetic origin for the ^{182}W isotope anomalies in OIB, which could not firmly be excluded in prior studies due to the observed correlated $\mu^{182}W$-$\mu^{183}W$ covariations (Mundl et al., 2017; Rizo et al., 2019). We also confirm that these anomalies are radiogenic.

4.3. Origin of ^{182}W Deficits in Ocean Island Basalts

A radiogenic origin of the ^{182}W deficits in OIB implies that their mantle source either had a low Hf/W ratio (relative to the BSE) established during the lifetime of ^{182}Hf (i.e., within the first ~60 Ma of Solar System history), or alternatively, the mantle source acquired ^{182}W deficits due to interaction with another source characterized by $\mu^{182}W < 0$. Prior studies have proposed that low Hf/W mantle reservoirs could have been formed by early differentiation events within the mantle (Mundl et al., 2017), but a lack of ^{142}Nd anomalies in OIB (Horan et al., 2018), which would be expected for a reservoir that underwent early silicate liquid-crystal fractionation, makes this scenario unlikely. Hence, interaction with a source characterized by strong ^{182}W deficits (i.e., $\mu^{182}W$ of *ca.* −200 or lower) is a more likely cause for ^{182}W anomalies present in OIB. Candidate sources include the core (Mundl-Petermeier et al., 2020; Rizo et al., 2019), which has an estimated $\mu^{182}W$ of ca. −220 (Kleine et al., 2004), and late-accreted material, which was added during the final ~0.5% of Earth's accretion and had an on average chondritic $\mu^{182}W$ of −190 (Kleine et al., 2004). How late-accreted materials have been distributed throughout the mantle over Earth's history is debated, but there is evidence that certain mantle sources lacked a "normal" (i.e., modern BSE-like) number of late-accreted materials (e.g., Archer et al., 2019; Dale et al., 2017; Puchtel et al., 2018; Willbold et al., 2011), while others were instead enriched in late-accreted materials (e.g., Puchtel et al., 2020). Consistent with this, Tolstikhin and Hofmann (2005) and Tolstikhin et al. (2006) proposed

that the base of the mantle may contain subducted Hadean crust that was loaded with a terrestrial regolith containing late-accreted materials with an on average chondritic composition. The terrestrial regolith containing metallic iron would have increased the density of the early formed crust, with a basalt/regolith ratio of 4:1, causing it to sink to the base of the mantle following subduction and stabilize to form the D″ layer. Thus, an alternative possibility to core-mantle interaction is that the ^{182}W deficits in OIB reflect an overabundance of late-accreted materials in their mantle sources.

One lingering issue for explaining ^{182}W anomalies by core-mantle interaction or an overabundance of late-accreted material is the lack of evidence for HSE enrichment in the mantle sources of OIB. For instance, the addition of only ∼0.2 wt.% of outer core metal to ambient mantle would produce a hybrid mantle with a μ^{182}W value of −18, but would also more than double its HSE content (Mundl et al., 2017). Simple mass balance reveals that addition of ∼0.9 wt.% of late-accreted materials to a reservoir with ambient mantle W characteristics would also produce a μ^{182}W value of −18 and HSE enrichment similar to the effect of direct addition of ∼0.2 wt. % of outer core material. To explain the HSE characteristics of OIB, some prior authors have argued that core-mantle interaction may have imposed core-derived W isotope signatures without significant HSE transfer by either exsolution of Si-Mg-Fe oxides from the core (Rizo et al., 2019), or W isotopic equilibration between a (partially) molten lower mantle layer and the core (Mundl-Petermeier et al., 2020; Rizo et al., 2019). However, first establishing whether or not OIB mantle sources are sufficiently enriched in HSE to be consistent with direct addition of core material or an overabundance of late accreted material is problematic, as the HSE contents of OIB mantle sources characterized by ^{182}W deficits are still poorly constrained. For example, because of the compatible behavior of HSE under partial melting conditions of OIB formation, only parental melt HSE abundances, rather than mantle source HSE abundances, have been accurately determined for Hawaiian OIB (e.g., Ireland et al., 2009). These parental melt HSE abundances cannot be directly related to mantle source HSE abundances because of the compatible to mildly incompatible behavior of HSE during partial melting and fractional crystallization of OIB (Ireland et al., 2009), and are insufficient to determine whether or not OIB mantle sources are enriched in HSE. Further, making comparisons between HSE abundances of OIB with other mantle-derived rocks is problematic because mantle-derived rocks with similar MgO contents have HSE abundances that vary by several orders of magnitude. As such, it is unlikely that a ∼2x increase in HSE abundances would be observable. Thus, direct addition of core material to the base of the mantle or an overabundance of late-accreted material remain equally viable explanations for ^{182}W deficits in some OIB, and based on available data, it is difficult to distinguish between these disparate interpretations.

An overabundance of late-accreted materials within the lower mantle could help explain the evolution of ^{182}W from the Archean mantle to the modern mantle. Archean mantle-derived rocks typically have μ^{182}W values of +10–15 (Archer et al., 2019 and references therein), and estimates of the HSE abundances within their mantle sources are typically only ∼30–80% of the modern upper mantle budget of HSE (e.g., Archer et al., 2019; Dale et al., 2017; Puchtel et al., 2018). These observations can be explained by a partial lack of late-accreted materials within Archean mantle sources (e.g., Archer et al., 2019; Dale et al., 2017; Puchtel et al., 2018; Willbold et al., 2011, 2015). Rizo et al. (2019) proposed that the entrainment of lower mantle materials with ^{182}W deficits could be responsible for the observed shift in the ^{182}W isotopic composition of the BSE since the Archean, but these authors preferred core-mantle interaction as the mechanism responsible for ^{182}W deficits. Alternatively, if the lowermost mantle has been an important reservoir of late-accreted materials, then continual entrainment of those materials within mantle plumes could also explain the evolution of ^{182}W of the BSE since the Archean.

4.4. Evidence From Combined Mo and W Isotopes of OIB

Mass-independent molybdenum isotope anomalies provide an additional tool to understand the origin of ^{182}W deficits in OIB. This is because, unlike the ^{182}W anomalies in OIB, Mo isotope variations are nucleosynthetic in origin and, as such, reflect the genetic heritage of the material from which Earth was built. The estimated Mo isotopic composition of the BSE is distinct from all known meteorites, which fall into either the NC or CC meteorite groups (e.g., Budde et al., 2019). In particular, the BSE Mo isotopic composition is intermediate between the NC and CC groups, indicating that the BSE's Mo derives from both the NC and CC reservoirs. The process that produced the BSE's mixed NC-CC Mo isotopic composition must have happened relatively late in Earth's accretion, as the Mo in the BSE reflects only the last 10%–20% of accretion (Dauphas, 2017). Thus, if nucleosynthetic anomalies are present in the mantle sources of some OIB due to the preservation of some of

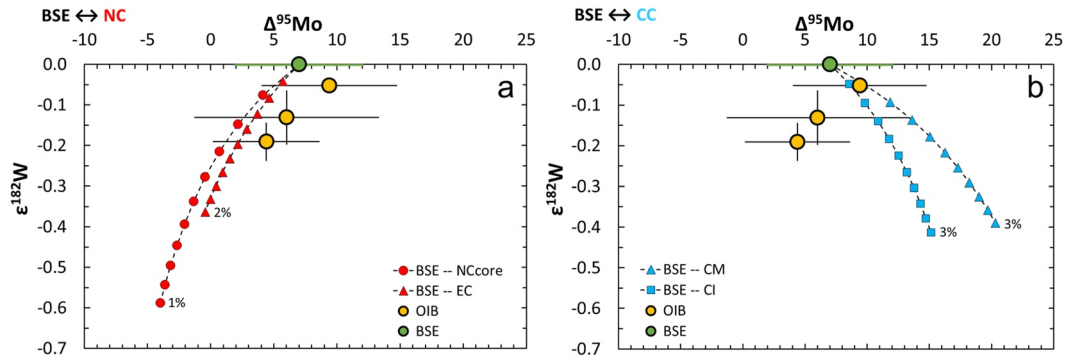

Figure 7. $\varepsilon^{182}W$ (part in 10,000 deviation of $^{182}W/^{184}W$ from a terrestrial standard) versus Mo isotopic compositions ($\Delta^{95}Mo = (\varepsilon^{95}Mo - 0.596 \times \varepsilon^{94}Mo) \times 100$) for Hawaiian ocean island basalts as well as mixing models between the BSE and candidate late accretion endmembers. Percentages of endmembers are shown at the end of each trend. (a) Endmember compositions include NC-like core and enstatite chondrites. (b) Endmember compositions include CM and CI carbonaceous chondrites. Parameters for BSE are from Arevalo and McDonough (2008), Budde et al. (2019), and Greber et al. (2015). Parameters for an NC-like core are from Budde et al. (2019), Li (2020), and Touboul et al. (2012). Molybdenum concentrations and Mo isotopic compositions for meteorite endmembers are from Burkhardt et al. (2011), Burkhardt et al. (2019), Spitzer et al. (2020), and references therein. Tungsten concentrations and isotopic compositions of meteorite endmembers from Braukmüller et al. (2018), Kleine et al. (2004), and Lee and Halliday (2000). See Text S2 in Supporting Information S1 for parameters and details of the mixing models, including concentrations used for model calculations.

Earth's later-stage building blocks, a significant difference in the Mo isotopic compositions of OIB and the BSE might exist. However, as shown in Figure 7, Hawaiian OIB have Mo isotopic compositions that instead overlap with an estimate of the BSE.

This lack of resolvable Mo anomalies provides constraints on the genetic heritage of the low-$\mu^{182}W$ component in OIB sources and in particular on whether this component has an NC- or CC-like heritage. For instance, for most elements investigated so far, the isotopic composition of Earth is most similar to enstatite chondrites, which belong to the NC group (e.g., Dauphas, 2017), indicating that although Earth's building material was likely isotopically heterogeneous, the average isotopic composition of this material is enstatite chondrite-like (Burkhardt et al., 2021). Thus, since almost all the Mo accreted by Earth resides in its core, it is reasonable to assume an enstatite chondrite-like Mo isotopic composition for the core. An enstatite chondrite-like isotopic composition has also been inferred for late-accreted material (Bermingham et al., 2018; Fischer-Gödde & Kleine, 2017; Worsham & Kleine, 2021). However, some studies also argue for a CI- or CM chondrite-like heritage of late-accreted material (Wang & Becker, 2013) and it has been suggested that this material was isotopically heterogeneous and unevenly distributed throughout the Earth's mantle (Fischer-Gödde et al., 2020).

To assess whether the combined W and Mo isotope data for OIB are consistent with either inferred compositions of the core or late-accreted material, we use a simple mixing model between ambient mantle and either the core or late-accreted materials (Figure 7). The data are consistent with an NC-like isotopic composition of the low-$\mu^{182}W$ component in the OIB sources, regardless of whether this component is Earth's core or late-accreted material. By contrast, the data are inconsistent with a purely CC-like heritage of the low-$\mu^{182}W$ component. Thus, if the ^{182}W deficits of OIB reflect an overabundance of late-accreted materials in their source, then this material must have an NC-like heritage, consistent with the most recent evidence for an NC heritage of late-accreted material (Worsham & Kleine, 2021). As such, the lack of nucleosynthetic Mo isotope variations is consistent with both core-mantle interaction and an overabundance of late-accreted materials at the base of the mantle as the origin of ^{182}W deficits in OIB, but only if these materials have an NC heritage.

5. Conclusions

This study confirms the presence of ^{182}W deficits in some OIB from Samoa and Hawaii reported in prior studies, and shows that there are no resolvable nucleosynthetic W or Mo isotope anomalies in these samples. As such, these data demonstrate that the ^{182}W deficits in OIB are purely radiogenic in origin, and that the hint of correlated ^{182}W–^{183}W variations among OIB observed in some prior datasets does not reflect nucleosynthetic isotope heterogeneity. Viable explanations for the radiogenic ^{182}W deficits include core-mantle interaction, either by

direct addition of core material or W isotopic diffusion, and a preserved overabundance of late-accreted materials in the source of OIB. The lack of nucleosynthetic Mo isotope anomalies in the OIB is consistent with both explanations, but only if the ^{182}W deficits are inherited from material with an NC-like isotopic composition. This in turn is consistent with the expected isotopic composition of Earth's core as well as with the most recent evidence for an NC heritage of the late-accreted material, but it would rule out a CC heritage of this material.

Data Availability Statement

The W and Mo isotope data used in this study are available at the TRR 170-DB Repository (https://doi.org/10.35003/YCUKOX).

Acknowledgments
Christoph Burkhardt is gratefully acknowledged for helpful conversations about this project. Rich Walker, Andi Mundl, the University of Maryland College Park, and the U.S. National Museum of Natural History (Smithsonian Institution, Washington, DC) are thanked for providing samples as well as fruitful discussions. This study was performed under the auspices of the U.S. Department of Energy by Lawrence Livermore National Laboratory under contract DE-AC52-07NA27344 with release number LLNL-JRNL-844238. This study was funded by the Deutsche Forschungsgemeinschaft (DFG, German Research Foundation) – Project-ID 263649064 – TRR 170. This is TRR 170 publication no. 183. Open Access funding enabled and organized by Projekt DEAL.

References

Andreasen, R., & Sharma, M. (2009). Fractionation and mixing in a thermal ionization mass spectrometer source. Implications and limitations for high precision Nd isotope analyses. *International Journal of Mass Spectrometry*, *285*(1–2), 49–57. https://doi.org/10.1016/j.ijms.2009.04.004

Archer, G. J., Brennecka, G. A., Gleissner, P., Stracke, A., Becker, H., & Kleine, T. (2019). Lack of late-accreted material as the origin of ^{182}W excesses in the Archean mantle: Evidence from the Pilbara Craton, Western Australia. *Earth and Planetary Science Letters*, *528*, 115841. https://doi.org/10.1016/j.epsl.2019.115841

Archer, G. J., Mundl, A., Walker, R. J., Worsham, E. A., & Bermingham, K. R. (2017). High precision analysis of ^{182}W/^{184}W and ^{183}W/^{184}W by negative thermal ionization mass spectrometry: Per-integration oxide corrections using measured ^{18}O/^{16}O. *International Journal of Mass Spectrometry*, *414*, 80–86. https://doi.org/10.1016/j.ijms.2017.01.002

Arevalo, R., Jr., & McDonough, W. F. (2008). Tungsten geochemistry and implications for understanding the Earth's interior. *Earth and Planetary Science Letters*, *272*(3–4), 656–665. https://doi.org/10.1016/j.epsl.2008.05.031

Bermingham, K. R., Walker, R. J., & Worsham, E. A. (2016). Refinement of high precision Ru isotope analysis using negative thermal ionization mass spectrometry. *International Journal of Mass Spectrometry*, *403*, 15–26. https://doi.org/10.1016/j.ijms.2016.02.003

Bermingham, K. R., Worsham, E. A., & Walker, R. J. (2018). New insights into Mo and Ru isotope variation in the nebula and terrestrial planet accretionary genetics. *Earth and Planetary Science Letters*, *487*, 221–229. https://doi.org/10.1016/j.epsl.2018.01.017

Braukmüller, N., Wombacher, F., Hezel, D. C., Escoube, R., & Münker, C. (2018). The chemical composition of carbonaceous chondrites: Implications for volatile element depletion, complementarity and alteration. *Geochimica et Cosmochimica Acta*, *239*, 17–48. https://doi.org/10.1016/j.gca.2018.07.023

Brennecka, G. A., Burkhardt, C., Budde, G., Kruijer, T. S., Nimmo, F., & Kleine, T. (2020). Astronomical context of Solar System formation from molybdenum isotopes in meteorite inclusions. *Science*, *370*(6518), 837–840. https://doi.org/10.1126/science.aaz8482

Budde, G., Archer, G., Tissot, F. L. H., Tappe, S., & Kleine, T. (2022). On the origin of analytical ^{183}W fractionation and its implications for tungsten isotope measurements. *Journal of Analytical Atomic Spectrometry*, *37*(10), 2005–2021. https://doi.org/10.1039/d2ja00102k

Budde, G., Burkhardt, C., & Kleine, T. (2019). Molybdenum isotopic evidence for the late accretion of outer Solar System material to Earth. *Nature Astronomy*, *3*(8), 736–741. https://doi.org/10.1038/s41550-019-0779-y

Budde, G., Kleine, T., Kruijer, T. S., Burkhardt, C., & Metzler, K. (2016). Tungsten isotopic constraints on the age and origin of chondrules. *Proceedings of the National Academy of Sciences*, *113*(11), 2886–2891. https://doi.org/10.1073/pnas.1524980113

Burkhardt, C., Borg, L. E., Brennecka, G. A., Shollenberger, Q. R., Dauphas, N., & Kleine, T. (2016). A nucleosynthetic origin for the Earth's anomalous ^{142}Nd composition. *Nature*, *537*(7620), 394–398. https://doi.org/10.1038/nature18956

Burkhardt, C., Dauphas, N., Hans, U., Bourdon, B., & Kleine, T. (2019). Elemental and isotopic variability in solar system materials by mixing and processing of primordial disk reservoirs. *Geochimica et Cosmochimica Acta*, *261*, 145–170. https://doi.org/10.1016/j.gca.2019.07.003

Burkhardt, C., Kleine, T., Dauphas, N., & Wieler, R. (2012). Nucleosynthetic tungsten isotope anomalies in acid leachates of the Murchison chondrite: Implications for hafnium–tungsten chronometry. *The Astrophysical Journal Letters*, *753*, 1–6. https://doi.org/10.1088/2041-8205/753/1/l6

Burkhardt, C., Kleine, T., Oberli, F., Pack, A., Bourdon, B., & Wieler, R. (2011). Molybdenum isotope anomalies in meteorites: Constraints on solar nebula evolution and origin of the Earth. *Earth and Planetary Science Letters*, *312*(3–4), 390–400. https://doi.org/10.1016/j.epsl.2011.10.010

Burkhardt, C., & Schönbächler, M. (2015). Intrinsic W nucleosynthetic isotope variations in carbonaceous chondrites: Implications for W nucleosynthesis and nebular vs. parent body processing of presolar materials. *Geochimica et Cosmochimica Acta*, *165*, 361–375. https://doi.org/10.1016/j.gca.2015.06.012

Burkhardt, C., Spitzer, F., Morbidelli, A., Budde, G., Render, J. H., Kruijer, T. S., & Kleine, T. (2021). Terrestrial planet formation from lost inner solar system material. *Science Advances*, *7*(52), eabj7601. https://doi.org/10.1126/sciadv.abj7601

Cook, D. L., & Schönbächler, M. (2016). High-precision measurement of W isotopes in Fe–Ni alloy and the effects from the nuclear field shift. *Journal of Analytical Atomic Spectrometry*, *31*(7), 1400–1405. https://doi.org/10.1039/c6ja00015k

Dale, C. W., Kruijer, T. S., & Burton, K. W. (2017). Highly siderophile element and ^{182}W evidence for a partial late veneer in the source of 3.8 Ga rocks from Isua, Greenland. *Earth and Planetary Science Letters*, *458*, 394–404. https://doi.org/10.1016/j.epsl.2016.11.001

Dauphas, N. (2017). The isotopic nature of the Earth's accreting material through time. *Nature*, *541*(7638), 521–524. https://doi.org/10.1038/nature20830

Fischer-Gödde, M., Elfers, B.-M., Münker, C., Szilas, K., Maier, W. D., Messling, N., et al. (2020). Ruthenium isotope vestige of Earth's pre-late veneer mantle. *Nature*, *579*(7798), 240–244. https://doi.org/10.1038/s41586-020-2069-3

Fischer-Gödde, M., & Kleine, T. (2017). Ruthenium isotopic evidence for an inner Solar System origin of the late veneer. *Nature*, *541*(7638), 525–527. https://doi.org/10.1038/nature21045

Greber, N. D., Puchtel, I. S., Näglera, T. F., & Mezger, K. (2015). Komatiites constrain molybdenum isotope composition of the Earth's mantle. *Earth and Planetary Science Letters*, *421*, 129–138. https://doi.org/10.1016/j.epsl.2015.03.051

Honda, M., McDougall, I., Patterson, D. B., Doulgeris, A., & Clague, D. A. (1991). Possible solar noble-gas component in Hawaiian basalts. *Nature*, *349*(6305), 149–151. https://doi.org/10.1038/349149a0

Horan, M. F., Carlson, R. W., Walker, R. J., Jackson, M., Garçon, M., & Norman, M. (2018). Tracking Hadean processes in modern basalts with 142-Neodymium. *Earth and Planetary Science Letters*, *484*, 184–191. https://doi.org/10.1016/j.epsl.2017.12.017

Ireland, T. J., Walker, R. J., & Garcia, M. O. (2009). Highly siderophile element and ^{187}Os isotope systematics of Hawaiian picrites: Implications for parental melt composition and source heterogeneity. *Chemical Geology*, *260*(1–2), 112–128. https://doi.org/10.1016/j.chemgeo.2008.12.009

Kleine, T., Mezger, K., Münker, C., Palme, H., & Bischoff, A. (2004). ^{182}Hf-^{182}W isotope systematics of chondrites, eucrites, and martian meteorites: Chronology of core formation and early mantle differentiation in Vesta and Mars. *Geochimica et Cosmochimica Acta*, *68*(13), 2935–2946. https://doi.org/10.1016/j.gca.2004.01.009

Kleine, T., Münker, C., Metzger, K., & Palme, H. (2002). Rapid accretion and early core formation on asteroids and the terrestrial planets from Hf-W chronometry. *Nature*, *418*(6901), 952–955. https://doi.org/10.1038/nature00982

Kruijer, T. S., Burkhardt, C., Budde, G., & Kleine, T. (2017). Age of Jupiter inferred from the distinct genetics and formation times of meteorites. *Proceedings of the National Academy of Sciences*, *114*(26), 6712–6716. https://doi.org/10.1073/pnas.1704461114

Kruijer, T. S., & Kleine, T. (2018). No ^{182}2W excess in the Ontong Java Plateau source. *Chemical Geology*, *458*, 24–31. https://doi.org/10.1016/j.chemgeo.2018.03.024

Kruijer, T. S., Kleine, T., Fischer-Gödde, M., Burkhardt, C., & Wieler, R. (2014). Nucleosynthetic W isotope anomalies and the Hf–W chronometry of Ca–Al-rich inclusions. *Earth and Planetary Science Letters*, *403*, 317–327. https://doi.org/10.1016/j.epsl.2014.07.003

Kruijer, T. S., Kleine, T., Fischer-Gödde, M., & Sprung, P. (2015). Lunar tungsten isotopic evidence for the late veneer. *Nature*, *520*(7548), 534–537. https://doi.org/10.1038/nature14360

Kruijer, T. S., Sprung, P., Kleine, T., Leya, I., Burkhardt, C., & Wieler, R. (2012). Hf-W chronometry of core formation in planetesimals inferred from weakly irradiated iron meteorites. *Geochimica et Cosmochimica Acta*, *99*, 287–304. https://doi.org/10.1016/j.gca.2012.09.015

Kurz, M. D., Jenkins, W. J., Hart, S. R., & Clague, D. (1983). Helium isotopic variations in volcanic rocks from Loihi Seamount and the Island of Hawaii. *Earth and Planetary Science Letters*, *66*, 388–406. https://doi.org/10.1016/0012-821x(83)90154-1

Lee, D.-C., & Halliday, A. N. (2000). Accretion of primitive planetesimals: Hf-W isotopic evidence from enstatite chondrites. *Science*, *288*(5471), 1629–1631. https://doi.org/10.1126/science.288.5471.1629

Li, J. (2020). Composition of the Earth's core. In S. Elias & D. Alderton (Eds.), *Encyclopedia of Geology* (2nd ed., pp. 1–14). Academic Press.

Lu, Q., & Masuda, A. (1994). The isotopic composition and atomic weight of molybdenum. *International Journal of Mass Spectrometry and Ion Processes*, *130*(1–2), 65–72. https://doi.org/10.1016/0168-1176(93)03900-7

Ludwig, K. R. (2001). *Users Manual for Isoplot/Ex version 2.47. A geochronological toolkit for Microsoft Excel*. Berkeley Geochronology Center Special Publication.

Mundl, A., Touboul, M., Jackson, M. G., Day, J. M. D., Kurz, M. D., Lekic, V., et al. (2017). Tungsten-182 heterogeneity in modern ocean island basalts. *Science*, *356*(6333), 66–69. https://doi.org/10.1126/science.aal4179

Mundl-Petermeier, A., Walker, R. J., Fischer, R. A., Lekic, V., Jackson, M. G., & Kurz, M. D. (2020). Anomalous ^{182}W in high ^{3}He/^{4}He ocean island basalts: Fingerprints of Earth's core? *Geochimica et Cosmochimica Acta*, *271*, 194–211. https://doi.org/10.1016/j.gca.2019.12.020

Nauret, F., Snow, J. E., Hellebrand, E., & Weis, D. (2011). Geochemical composition of K-rich lavas from the Lena Trough (Arctic Ocean). *Journal of Petrology*, *52*(6), 1185–1206. https://doi.org/10.1093/petrology/egr024

Puchtel, I. S., Blichert-Toft, J., Touboul, M., & Walker, R. J. (2018). ^{182}W and HSE constraints from 2.7 Ga komatiites on the heterogeneous nature of the Archean mantle. *Geochimica et Cosmochimica Acta*, *228*, 1–26. https://doi.org/10.1016/j.gca.2018.02.030

Puchtel, I. S., Mundl-Petermeier, A., Horan, M., Hanski, E. J., Blichert-Toft, J., & Walker, R. J. (2020). Ultradepleted 2.05 Ga komatiites of Finnish Lapland: Products of grainy late accretion or core-mantle interaction? *Chemical Geology*, *554*, 119801. https://doi.org/10.1016/j.chemgeo.2020.119801

Qin, L., Dauphas, N., Wadhwa, M., Markowski, A., Gallino, R., Janney, P. E., & Bouman, C. (2008). Tungsten nuclear anomalies in planetesimal cores. *The Astrophysical Journal*, *674*(2), 1234–1241. https://doi.org/10.1086/524882

Rizo, H., Andrault, D., Bennett, N. R., Humayun, M., Brandon, A., Vlastelic, I., et al. (2019). ^{182}W evidence for core-mantle interaction in the source of mantle plumes. *Geochemical Perspectives Letters*, *11*, 6–11. https://doi.org/10.7185/geochemlet.1917

Spitzer, F., Burkhardt, C., Budde, G., Kruijer, T. S., Morbidelli, A., & Kleine, T. (2020). Isotopic evolution of the inner Solar System inferred from molybdenum isotopes in meteorites. *The Astrophysical Journal Letters*, *898*(1), L2. https://doi.org/10.3847/2041-8213/ab9e6a

Takamasa, A., Suzuki, K., Fukami, Y., Iizuka, T., Tejada, M. L. G., Fujisaki, W., et al. (2020). Improved method for highly precise and accurate ^{182}W/^{184}W isotope measurements by multiple collector inductively coupled plasma mass spectrometry and application for terrestrial samples. *Geochemical Journal*, *54*(3), 117–127. https://doi.org/10.2343/geochemj.2.0594

Tolstikhin, I. N., & Hofmann, A. W. (2005). Early crust on top of the Earth's core. *Physics of the Earth and Planetary Interiors*, *148*(2–4), 109–130. https://doi.org/10.1016/j.pepi.2004.05.011

Tolstikhin, I. N., Kramers, J. D., & Hofmann, A. W. (2006). A chemical Earth model with whole mantle convection: The importance of a core–mantle boundary layer (D″) and its early formation. *Chemical Geology*, *226*(3–4), 79–99. https://doi.org/10.1016/j.chemgeo.2005.09.015

Touboul, M., Puchtel, I. S., & Walker, R. J. (2012). ^{182}W evidence for long-term preservation of early mantle differentiation products. *Science*, *335*(6072), 1065–1069. https://doi.org/10.1126/science.1216351

Vermeesch, P. (2018). IsoplotR: A free and open toolbox for geochronology. *Geoscience Frontiers*, *9*(5), 1479–1493. https://doi.org/10.1016/j.gsf.2018.04.001

Wang, Z., & Becker, H. (2013). Ratios of S, Se and Te in the silicate Earth require volatile-rich late veneer. *Nature*, *499*(7458), 328–331. https://doi.org/10.1038/nature12285

Willbold, M., Elliott, T., & Moorbath, S. (2011). The tungsten isotopic composition of the Earth's mantle before the terminal bombardment. *Nature*, *477*(7363), 195–198. https://doi.org/10.1038/nature10399

Willbold, M., Mojzsis, S. J., Chen, H. W., & Elliott, T. (2015). Tungsten isotope composition of the Acasta Gneiss Complex. *Earth and Planetary Science Letters*, *419*, 168–177. https://doi.org/10.1016/j.epsl.2015.02.040

Worsham, E. A., Burkhardt, C., Budde, G., Fischer-Gödde, M., Kruijer, T. S., & Kleine, T. (2019). Distinct evolution of the carbonaceous and non-carbonaceous reservoirs: Insights from Ru, Mo, and W isotopes. *Earth and Planetary Science Letters*, *521*, 103–112. https://doi.org/10.1016/j.epsl.2019.06.001

Worsham, E. A., & Kleine, T. (2021). Late accretionary history of Earth and Moon preserved in lunar impactites. *Science Advances*, *7*(44), 1–10. https://doi.org/10.1126/sciadv.abh2837